Acta Crystallographica Section B
**Structural Science**
ISSN 0108-7681

# High-precision absolute lattice parameter determination of $SrTiO_3$, $DyScO_3$ and $NdGaO_3$ single crystals

**Martin Schmidbauer,* Albert Kwasniewski and Jutta Schwarzkopf**

Leibniz Institute for Crystal Growth, Max-Born-Str. 2, D-12489 Berlin, Germany

Correspondence e-mail: schmidbauer@ikz-berlin.de

Received 22 July 2011
Accepted 5 November 2011

The lattice parameters of three perovskite-related oxides have been measured with high precision at room temperature. An accuracy of the order of $10^{-5}$ has been achieved by applying a sophisticated high-resolution X-ray diffraction technique which is based on the modified Bond method. The results on cubic $SrTiO_3$ [$a$ = 3.905268 (98) Å], orthorhombic $DyScO_3$ [$a$ = 5.442417 (54), $b$ = 5.719357 (52) and $c$ = 7.904326 (98) Å], and orthorhombic $NdGaO_3$ [$a$ = 5.428410 (54), $b$ = 5.498407 (55) and $c$ = 7.708878 (95) Å] are discussed in view of possible systematic errors as well as non-stoichiometry in the crystals.

## 1. Introduction

In recent years complex oxide epitaxial thin films have attracted considerable interest owing to their potential applications in oxide electronics. Defined strain states in such oxide films are of particular interest since they can alter or even fundamentally change their ferroelectric, ferromagnetic, multiferroic and superconducting properties. For example, it has been demonstrated that incorporation of biaxial strain into $SrTiO_3$ and $BaTiO_3$ thin films may dramatically enhance the ferroelectric transition temperature, and values far above room temperature were reached (Haeni *et al.*, 2004; Choi *et al.*, 2004).

Although a variety of sophisticated techniques has been described, *e.g.* Eerenstein *et al.* (2007), Moram *et al.* (2007) and Biegalski *et al.* (2010), a defined strain state in films is usually achieved by growing them on different suitable substrates exhibiting different in-plane lattice parameters with respect to the thin films. Coherent (pseudomorphic) epitaxial growth then leads to biaxial strain in the films, which scales with the in-plane lattice mismatch between the thin film and the substrate material. Depending on the sign of the lattice mismatch the thin films are compressively or tensile strained. For example, for $SrRuO_3$ thin films – a material which is often used as the bottom electrode for a variety of ferroelectric and multiferroic thin film heterostructures, *e.g.* Marimoto *et al.* (2000), Boikov & Claeson (2001), Sim *et al.* (2006), and Yuan & Uedono (2009) – a shift in the Curie temperature ($T_C$) of the ferromagnetic phase transition has been observed when the thin films were grown on substrates exhibiting different lattice mismatches to the film. It was found that $T_C$ increases with tensile strain and decreases with compressive strain. These conditions can be achieved by using $NdGaO_3$, $DyScO_3$ and $SrTiO_3$ single crystals as substrates (Dirsyte *et al.*, 2011).

A detailed knowledge of the lattice mismatch between different epitaxial films and the underlying substrate is thus absolutely essential to tune the strain state in coherently grown epitaxial layers and – in a next step – to study the

impact of strain on the functional properties of complex oxide thin films. Moreover, in most cases strains in epitaxial layers are experimentally determined by high-resolution X-ray diffraction techniques. Here the relative angular positions of the layer and substrate Bragg peaks are used to evaluate the elastic strains in the film. The accurate evaluation of small strains in layers grown on substrates again requires a precise knowledge of the substrate lattice parameters.

In this study we have selected the materials $DyScO_3$, $NdGaO_3$ and $SrTiO_3$. Beyond their important role as substrates for the epitaxial growth of a variety of technologically relevant complex oxide thin films and high-temperature superconductors these materials also exhibit interesting physical properties. Plenty of work has been spent in the determination of the crystal structure of $DyScO_3$, $NdGaO_3$ and $SrTiO_3$. At room temperature $SrTiO_3$ is a centrosymmetric cubic perovskite material (space group *Pm3m*) while $DyScO_3$ and $NdGaO_3$ exhibit a distorted orthorhombic (pseudo-perovskite) crystal structure with respective space groups (at room temperature) *Pbnm* ($Z$ = 4) for $NdGaO_3$ (Vasylechko *et al.*, 2000) and *Pnma* ($Z$ = 4) for $DyScO_3$ (Velickov *et al.*, 2007). Most of these studies are based on the evaluation of X-ray/neutron powder diffraction patterns or single-crystal diffraction patterns using a two-dimensional detector system. For these techniques a large number of Bragg reflections, which serves as input for Rietveld refinement procedures (Rietveld, 1969), is available; the relative intensities of the Bragg reflections are used to refine the atomic positions inside the unit cell. However, for powder and single-crystal diffraction the absolute precision in the determination of the Bragg angles is often restricted, which yields comparatively large errors for the unit-cell dimensions. Any misalignment of the sample (*e.g.* the illuminated sample volume does not contain the main axis of rotation) will lead to systematic errors in the determination of the Bragg angles. This is probably the reason why the values for the *a*, *b* and *c* lattice parameters of $DyScO_3$ (Clark *et al.*, 1978; Liferovich & Mitchell, 2004; Velickov *et al.*, 2007; Gesing, 2011) and $NdGaO_3$ (Geller, 1957; Marti *et al.*, 1994; Ubizskii *et al.*, 1994; Vasylechko *et al.*, 2000; Senyshyn *et al.*, 2009) reported so far vary over a rather large interval. On the other hand, it is also striking that the reported experimental errors for *a*, *b* and *c* in these works are often quite small. We suppose that these small error values have been estimated by the accuracy of the Rietveld refinement procedure while possible systematic errors given by the specific experimental set-up were not modelled with sufficiently high accuracy. However, it has been of major interest in these studies to analyse the atomic species and positions inside the unit cell while the precise determination of the unit-cell dimensions, *i.e.* the lattice parameters *a*, *b* and *c*, have not been the main focus.

We have already stressed that precise knowledge of the lattice parameters of $DyScO_3$, $NdGaO_3$ and $SrTiO_3$ is highly desirable since this would enable an accurate determination of the strain states of epitaxial films grown on these substrates. On the other hand, additional sources for lattice parameter changes such as

(i) deviations from exact stoichiometry,
(ii) the appearance of structural defects and
(iii) impurities in the crystals

could be studied and compared with corresponding model calculations. The aim of the present study is an accurate determination of the lattice parameters of $SrTiO_3$, $DyScO_3$ and $NdGaO_3$ single crystals. We have applied a sophisticated high-resolution X-ray technique which enabled us to measure the lattice parameters with an absolute accuracy of better than $2 \times 10^{-5}$, which is – to our knowledge – about one order of magnitude better than the best values reported as yet for these materials. We will present our results and compare them with results published in other works.

## 2. Sample preparation

The $DyScO_3$ bulk crystals have been grown at the Leibniz Institute for Crystal Growth using the conventional Czochralski technique. A detailed description of the fabrication process is given by Uecker *et al.* (2006), Velickov *et al.* (2007) and Uecker *et al.* (2008). Pieces of $\sim 5 \times 5 \times 0.5$ mm size were prepared. High-quality $SrTiO_3$ and $NdGaO_3$ single crystals were provided by the Company CrysTec. Pieces of $\sim 10 \times 10 \times 0.5$ mm size were used. For $SrTiO_3$ we have chosen (100) oriented crystals, while for $DyScO_3$ and $NdGaO_3$ the crystallographic orientations (110) and (001) have been selected for each material. The experimental full widths at half-maximum (FWHM) $\Delta\omega$ of the X-ray rocking curves were of the same order of magnitude as the instrumental resolution ($\Delta\omega$ = 11 arcsec) which proves the very high quality of the crystals. From the FWHMs an upper limit for the dislocation density of $\sim \rho = 10^5$ cm$^{-2}$ can be estimated (Dunn & Koch, 1957; Kaganer *et al.*, 2005), which is in agreement with the measured etch-pit density (not shown here).

## 3. Absolute lattice parameter determination

### 3.1. Experimental set-up

As already stated, a very common way to determine strains in epitaxial layers is the measurement of X-ray rocking curves. Here, a well characterized substrate serves as a 'lattice parameter standard', and a quantitative comparison of the angular positions of the layer and substrate Bragg peaks is used to determine the lattice parameter(s) of the layer. This indirect method thus represents a 'relative lattice parameter determination'. However, a variety of other X-ray techniques has been proposed for the absolute determination of the lattice parameters. A very useful overview and discussion about the applicability of these techniques to single crystalline and polycrystalline samples has been presented by Fewster (1999).

The experimental triple-axis setup used in this work is schematically shown in Fig. 1. The X-rays emitted from a sealed copper anode (working at typically 40 kV, 40 mA) are pre-collimated by a parabolic multilayer mirror (Schuster & Göbel, 1995) and then pass a four-bounce Bartels monochromator (Bartels, 1983) using the 220 Bragg reflections of

two highly perfect germanium channel-cut crystals. The X-ray beam is collimated down to the intrinsic Darwin width of the Ge 220 Bragg reflection of *ca* $\Delta\theta_D = 11$ arcsec = 0.003° = $5.3 \times 10^{-5}$ rad, while the Cu $K\alpha_1$ line is selected within a wavelength band of $\Delta\lambda/\lambda = 1.28 \times 10^{-4}$. The average wavelength of Cu $K\alpha_1$ radiation, $\lambda = 1.54059292\ (45)$ Å, is known with high accuracy (Härtwig *et al.*, 1993) which is better than the natural width of the line. However, the tuneable set-up of the Bartels monochromator with two Ge 220 channel-cut crystals may include some remaining uncertainty. We have therefore determined the X-ray wavelength by using a highly pure silicon standard substrate ($a_{Si} = 5.43102064$ Å) and obtained a value of $\lambda = (1.54059 \pm 0.00002)$ Å, which is in reasonable agreement with the value obtained by Härtwig *et al.* (1993). The temperature during the measurements was fixed to $T = (293 \pm 0.5)$ K and the mechanical stability of the monochromator was checked at regular intervals by measuring the intensity of the primary beam. During the entire measurement period we could not observe any long-term drift in the X-ray wavelength.

The use of a four-bounce Bartels monochromator ensures that the Bragg reflections of the samples are not broadened by wavelength dispersion (DuMond, 1937; Ayers & Ladell, 1988). The actual width of the rocking curves is given by the divergence of the incident beam (11 arcsec) and the inherent width of the sample Bragg reflection under investigation.

In front of a single-channel scintillation detector a two-bounce 220 germanium channel-cut crystal analyser is mounted which measures the direction ($2\theta$) of the diffracted beam with an accuracy of 11 arcsec.

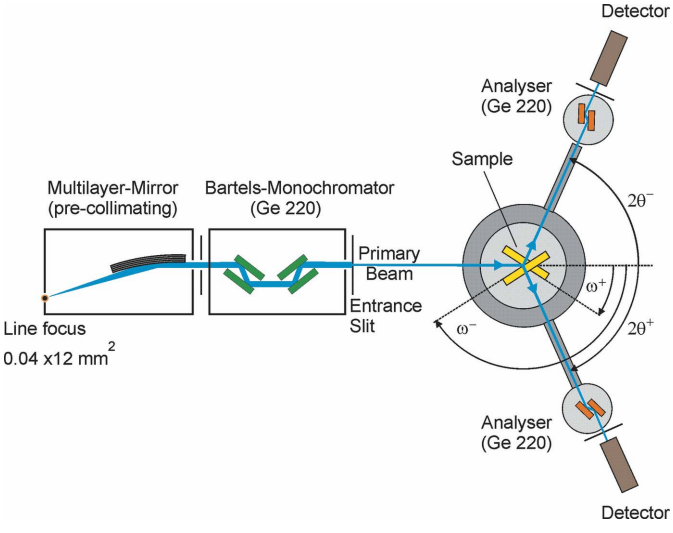


**Figure 1**
Schematic drawing of the experimental setup including the pre-collimating parabolic multilayer mirror, the Ge 220 Bartels monochromator, the sample stage and the Ge 220 analyser mounted on the detector stage. Two complementary sample ($\omega^+$, $\omega^-$) and detector ($2\theta^+$, $2\theta^-$) positions are shown to illustrate the extended Bond technique.

### 3.2. Modified Bond method

For a fixed Bragg reflection two complementary sample angular positions $\omega^+$ and $\omega^-$ are measured (Fig. 1), and the corresponding Bragg angle $\theta_B$ is then given by

$$\theta_B = \frac{1}{2}\left(180^\circ - (\omega^+ - \omega^-)\right). \quad (1)$$

Thus, any uncertainty in the zero position of the sample rotation has been eliminated since only the difference $\omega^+ - \omega^-$ in the measured angular positions determines the final result for the Bragg angle $\theta_B$. A precise reading of angular positions is ensured by optical encoders which guarantee a reproducible absolute accuracy of 0.00005 and 0.00010° for the sample ($\omega$) and the detector ($2\theta$) goniometers.

The described procedure – also known as the Bond method (Bond, 1960) – works well for perfect single crystals with narrow Bragg reflections. Possible eccentricity errors are eliminated and there is no need to measure the angular zero position of the sample. However, any sample imperfection caused by *e.g.* a slight crystal bending or mosaicity could dramatically reduce the accuracy of this method. In order to avoid this error sources and to cross-check the reliability of our measurements the directions of the diffracted beams with respect to the primary beam, $2\theta^+$ and $2\theta^-$, are measured by the analyser crystal with high accuracy simultaneously with the respective sample positions $\omega^+$ and $\omega^-$ (see Fig. 1). From these measurements the Bragg angle can then be calculated *via*

$$\theta_B = \frac{1}{4}\left(2\theta^+ - 2\theta^-\right). \quad (2)$$

Again, since only the difference $2\theta^+ - 2\theta^-$ is in the formula any uncertainty in the zero position of the analyser crystal will be eliminated. Even more importantly, a possible eccentricity error of the sample position with respect to the goniometer axis – which always has to be taken into account in powder diffraction setups by applying the so-called 'absorption correction' – will have no impact on the measured $2\theta^+$ and $2\theta^-$ values. For perfect crystals the evaluation of $\omega$ and $2\theta$ values should lead to identical results. In our experiment we found typical deviations of the order $\Delta\theta_B = 0.002^\circ = 3.5 \times 10^{-5}$ rad which determines the accuracy of our method. In the data evaluation procedure for the lattice spacings (§4) we separately evaluated our data based on the relationships in (1) and (2).

### 3.3. Experimental procedure and data evaluation

The number $N$ of Bragg reflections investigated in this study is less than the number usually achieved in powder diffraction analysis where typically hundreds of Bragg reflections are studied. In powder diffraction a large number of reflections is necessary in order to determine the electron density inside the unit cell with a high spatial resolution and to reduce the overall statistical error. On the other hand, the precise determination of the $a$, $b$ and $c$ lattice parameters using the Bond technique requires a far smaller number of (independent) Bragg reflections. $N = 4$ for $SrTiO_3$ and $N = 20$ for

**Table 1**
Critical angle of the total external reflection $\alpha_C$, refractive index parameters $\delta$, and surface roughness $\sigma$ for $SrTiO_3$, $DyScO_3$ and $NdGaO_3$ measured at $\lambda = 1.54059$ Å.

For comparison, the calculated refractive index parameters $\delta_{cal}$ using the data by Henke *et al.* (1993) are also presented.

| Crystal | $\alpha_C$ (°) | $\delta$ ($\times 10^5$) | $\delta_{cal}$ ($\times 10^5$) | $\sigma$ (nm) |
|---|---|---|---|---|
| $SrTiO_3$ | 0.326 | $1.52 \pm 0.10$ | 1.50 | 1.32 |
| $DyScO_3$ | 0.351 | $1.87 \pm 0.11$ | 1.77 | 1.45 |
| $NdGaO_3$ | 0.365 | $2.03 \pm 0.11$ | 2.06 | 1.26 |

$DyScO_3$/$NdGaO_3$ turned out to be sufficient to obtain an accuracy in the low $10^{-5}$ region.

It is well known from many other studies, *e.g.* Bond (1960), that a very crucial error source in determining the exact Bragg angle is given by a sample misalignment where the diffracting plane deviates from the diffractometer plane by a finite angle $\Delta\chi$. This error shifts the Bragg reflection (*hkl*) by

$$\Delta(2\theta_{hkl}) \simeq -\Delta\chi^2 \tan\theta_{hkl} \cos^2\tau, \tag{3}$$

where $\tau$ is the angle between the scattering vector and the crystal surface normal (Bond, 1960). From (3) and by using Bragg's law we can calculate the corresponding uncertainty of the lattice spacing

$$\begin{aligned}\Delta d_{hkl}/d_{hkl} &= -\cot\theta_{hkl}\Delta\theta_{hkl} \\ &= \frac{1}{2}\Delta\chi^2 \cot\theta_{hkl}\tan\theta_{hkl}\cos^2\tau = \frac{1}{2}\Delta\chi^2\cos^2\tau,\end{aligned} \tag{4}$$

which is independent of the Bragg angle. In order to minimize the 'tilt-error' we have carefully adjusted the sample for each Bragg reflection. Since the measured Bragg reflections are very narrow the tilt angle can be determined very precisely and an accuracy of better than $\Delta\chi = 0.1°$ has been achieved for all samples and Bragg reflections. For $\tau = 0$ this gives an upper limit for the relative error of $\Delta d_{hkl}/d_{hkl} = 1.5 \times 10^{-6}$.

For each Bragg reflection (*hkl*) the angular positions of the sample ($\omega^+$, $\omega^-$) and of the detector ($2\theta^+$, $2\theta^-$) were measured at least three times in order to check the reproducibility and to reduce the statistical error. The exact peak positions were determined by performing peak fits using Gaussian line profiles. An example is shown in Fig. 2 for the $006^-$ Bragg reflection of an (001)-oriented $NdGaO_3$ single crystal.

In a next step, the experimentally determined values for $\omega^+$, $\omega^-$, $2\theta^+$ and $2\theta^-$ were corrected for refraction. Fewster & Andrew (1998) have shown that refraction of the incident and diffracted wave at the sample surface shifts the experimental values by

$$\Delta(2\theta_{hkl}) = \delta[\cot\omega_{hkl} + \cot(2\theta_{hkl} - \omega_{hkl}) + \tan\theta_{hkl}] \tag{5a}$$

$$\Delta(\omega_{hkl}) = \delta[\cot\omega_{hkl} + \tan\theta_{hkl}], \tag{5b}$$

where $n = 1 - \delta$ is the real part of the complex refractive index, $\omega_{hkl}$ is the angle of the incident X-ray beam to the sample surface, and $\theta_{hkl}$ is the Bragg angle of the *hkl* reflection under study. Although tabulated values can be found in the literature (*e.g.* Henke *et al.*, 1993), we have independently determined $\delta$ by measuring the X-ray reflectivity in the vicinity of the regime of the total external reflection. Fig. 3 shows the measured reflectivity for a $DyScO_3$ substrate, together with the corresponding simulation using dynamical diffraction theory. From these simulations the critical angle of the total external reflection $\alpha_C$ can be determined, a quantity which is connected to the real part of the refractive index *via* (*e.g.* Als-Nielsen & McMorrow, 2001)

$$\alpha_C = (2\delta)^{1/2}. \tag{6}$$

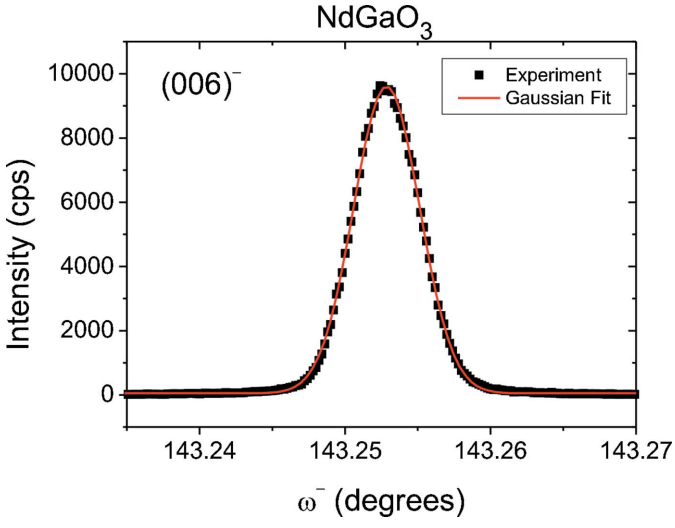


**Figure 2**
Experimental (black squares) rocking curve ($\omega$ scan) of the $(006)^-$ Bragg reflection of an $NdGaO_3$ (001) single crystal along with a Gaussian line fit (red line). The measured FWHM is $\Delta\omega = 0.0055°$. This figure is in colour in the electronic version of this paper.

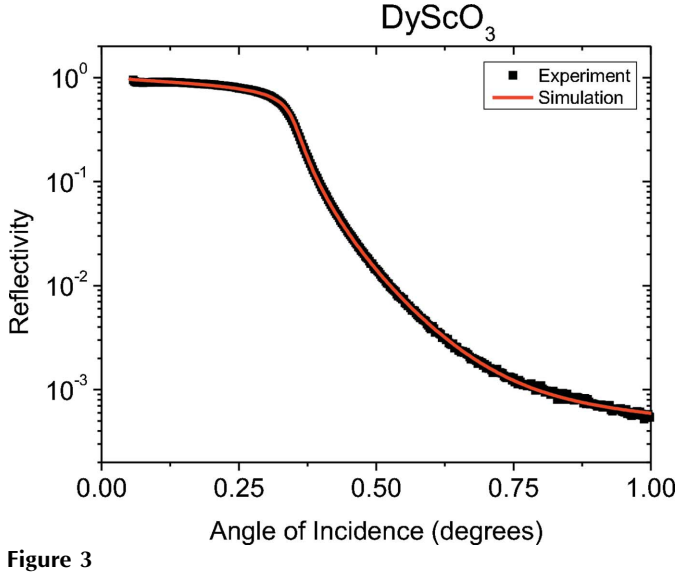


**Figure 3**
Experimental X-ray reflectivity (black squares) along with simulation (red line) for a $DyScO_3$ (110) substrate as a function of the glancing angle of incidence. The corresponding values for the refractive index and the critical angle of total external reflections are given in Table 1. This figure is in colour in the electronic version of this paper.

**Table 2**
Experimental lattice parameters *a*, *b* and *c*, and unit-cell volumes *V* of cubic $SrTiO_3$ and orthorhombic $DyScO_3$, and $NdGaO_3$ measured at room temperature in comparison with earlier work.

For evaluation of the mean values of previously published works the results obtained by Brous *et al.* (1953), Lytle (1964) and Geller (1957) have been omitted since the accuracy is not high enough or not comparable to the other results. XP: X-ray powder diffraction; NP: neutron powder diffraction; XS: X-ray single-crystal diffraction.

| Substrate | *a* (Å) | *b* (Å) | *c* (Å) | *V* (Å$^3$) | Experimental method |
|---|---|---|---|---|---|
| $SrTiO_3$ | 3.905268 (98) | | | 59.56[a] | |
| | 3.90631 (8) | | | 59.61[b] | XP |
| | 3.9053 | | | 59.56[c] | XP |
| | 3.899 | | | 59.27[d] | XP |
| | 3.901 (1) | | | 59.36[e] | XP |
| | 3.905 | | | 59.55[f] | XS |
| Mean value | 3.9042 | | | 59.51 | |
| $DyScO_3$ | 5.442417 (54) | 5.719357 (52) | 7.904326 (98) | 246.04[a] | |
| | 5.440 (1) | 5.716 (1) | 7.903 (1) | 245.74[g] | XP |
| | 5.4494 (1) | 5.7263 (1) | 7.9132 (1) | 246.93[h] | XP |
| | 5.4490 | 5.7273 | 7.9116 | 246.91[i] | XP |
| | 5.440 (1) | 5.717 (1) | 7.903 (1) | 245.86[j] | XP |
| | 5.443 (2) | 5.717 (2) | 7.901 (2) | 245.86[j] | XS |
| Mean value | 5.44428 | 5.72072 | 7.90636 | 246.24 | |
| $NdGaO_3$ | 5.428410 (54) | 5.498407 (55) | 7.708878 (95) | 230.09[a] | |
| | 5.42817 (9) | 5.49768 (9) | 7.70817 (13) | 230.03[k] | XP, NP |
| | 5.4276 (1) | 5.49790 (9) | 7.7078 (1) | 230.00[l] | XS |
| | 5.4276 (1) | 5.4979 (1) | 7.7078 (2) | 230.00[m] | XP |
| | 5.4333 (2) | 5.5036 (2) | 7.7157 (3) | 230.72[n] | NP |
| | 5.426 | 5.502 | 7.706 | 232.07[o] | XP |
| Mean value | 5.42969 | 5.49972 | 7.71055 | 230.25 | |

References: (*a*) this work, (*b*) Tkach *et al.* (2008), (*c*) Jeon *et al.* (1998), (*d*) Brous *et al.* (1953), (*e*) Abramov *et al.* (1995), (*f*) Lytle (1964), (*g*) Gesing (2011), (*h*) Liferovich & Mitchell (2004), (*i*) Clark *et al.* (1978), (*j*) Velickov *et al.* (2007), (*k*) Senyshyn *et al.* (2009), (*l*) Vasylechko *et al.* (2000), (*m*) Ubizskii *et al.* (1994), (*n*) Marti *et al.* (1994) and (*o*) Geller (1957).

The corresponding $\delta$ values obtained for $SrTiO_3$, $DyScO_3$ and $NdGaO_3$ are listed in Table 1 and fair agreement with calculated values using the data tables from Henke *et al.* (1993) is achieved.

After applying the refraction corrections (5) to the experimental quantities $\omega^+$, $\omega^-$, $2\theta^+$ and $2\theta^-$ the corresponding Bragg angles $\theta_{hkl}$ were calculated using (1) and (2) and are transposed to *d* values using the Bragg equation

$$d_{hkl} = \lambda/(2\sin\theta_{hkl}). \tag{7}$$

For an orthorhombic crystal these are connected to the lattice parameters *a*, *b* and *c* *via*

$$1/d_{hkl}^2 = h^2/a^2 + k^2/b^2 + l^2/c^2. \tag{8}$$

The experimental values of $d_{hkl}$ have been evaluated independently using (1) and (2). The respective results are listed in Table S1 (for $SrTiO_3$), Table S2 (for $DyScO_3$) and Table S3 (for $NdGaO_3$) of the supplementary material.[1] We have used a refinement procedure from which the lattice parameters *a*, *b* and *c* can be determined from (8). This was achieved by minimizing the normalized deviation, *S*, of the weighted absolute differences between calculated and measured lattice spacings

$$S = \frac{1}{[N(N-1)]^{1/2}} \sum_{h,k,l} w_{hkl} \frac{\left|d_{hkl}^{\rm exp} - d_{hkl}^{\rm cal}\right|}{d_{hkl}^{\rm exp}} = \frac{1}{[N(N-1)]^{1/2}} \sum_{h,k,l} w_{hkl} S_{hkl}, \tag{9}$$

where $d_{hkl}^{\rm exp}$ and $d_{hkl}^{\rm cal}$ are the experimentally derived and refined values for the lattice spacing of lattice plane (*hkl*) and *N* is the number of Bragg reflections under consideration. In order to account for uncertainties in determining the position of the Bragg peaks caused by restricted counting statistics (positive) weighting factors $w_{hkl}$ are introduced. They are proportional to the peak intensity (counts) of the measured Bragg reflections and they fulfil the relationship $\sum_{hkl} w_{hkl} = 1$. Strong Bragg reflections with reliable counting statistics thus give a significantly larger contribution to *S* compared with weak Bragg reflections with reduced counting statistics. Typical deviations $\left|d_{hkl}^{\rm exp} - d_{hkl}^{\rm cal}\right|/d_{hkl}^{\rm exp}$ for the individual Bragg reflections are of the order $10^{-5}$, proving the high accuracy of our method (see Tables S2, S3 and S4). In order to evaluate the lattice parameters *a*, *b* and *c*, and unit-cell volumes *V*, averaged values received from the $\omega$ and $2\theta$ measurements have been used.

## 4. Results and discussion

In Table 2 our results are listed along with experimental results from other selected published works. On first sight, the lattice parameters obtained for $SrTiO_3$, $DyScO_3$ and $NdGaO_3$ do not agree very well with previous studies within the accuracy ($2 \times 10^{-5}$) of the present study. In order to compare our data in more detail with previously published work we have determined the mean values for the lattice parameters by averaging the values of selected published data. The relative deviations between these mean values and our values are in the low $10^{-4}$ regime (see Table 2), while the relative scattering (standard deviation) among the data from other works is of the same order of magnitude. Nevertheless, the experimental errors for the lattice parameters as listed in Table 2 for previous works are quite small. These errors are presumably determined by the accuracy of the Rietveld refinement procedure, *i.e.* only statistical errors were considered while systematic errors were not modelled with sufficiently high accuracy. The observed deviations between our study and former works could thus be a result of systematic experimental errors in the previous studies which might be quite large for X-ray/neutron powder diffraction or single-crystal X-ray diffraction. However, we again have to emphasize here that most of the previously published works were optimized for structural analysis inside the unit cell, while the unit-cell dimensions were of secondary interest only. On the other hand the experimental technique applied in our work, which is based on the modified Bond method, is very accurate for the absolute determination of lattice parameters, and an upper

[1] Supplementary data for this paper are available from the IUCr electronic archives (Reference: KD5054). Services for accessing these data are described at the back of the journal.

**Table 3**
Experimental aspect ratios for lattice parameters $a$, $b$ and $c$ of orthorhombic $DyScO_3$ and $NdGaO_3$ measured at room temperature compared with earlier work.

For evaluation of the mean values of previous work the results obtained by Geller (1957) have been omitted.

| Substrate | $a/c$ | $b/c$ | $a/b$ |
|---|---|---|---|
| $DyScO_3$ | 0.68854 | 0.72357 | 0.95158[a] |
| | 0.68835 | 0.72327 | 0.95171[b] |
| | 0.68864 | 0.72363 | 0.95164[c] |
| | 0.68874 | 0.72391 | 0.95141[d] |
| | 0.68890 | 0.72358 | 0.95207[e] |
| Mean value | 0.68866 | 0.72360 | 0.95171 |
| $NdGaO_3$ | 0.70418 | 0.71326 | 0.98727[a] |
| | 0.70421 | 0.71323 | 0.98736[f] |
| | 0.70417 | 0.71329 | 0.98721[g] |
| | 0.70417 | 0.71329 | 0.98721[h] |
| | 0.70419 | 0.71330 | 0.98723[i] |
| | 0.70413 | 0.71399 | 0.98619[j] |
| Mean value | 0.70419 | 0.71328 | 0.98725 |

References: (*a*) this work, (*b*) Gesing (2011), (*c*) Liferovich & Mitchell (2004), (*d*) Clark *et al.* (1978), (*e*) Velickov *et al.* (2007), (*f*) Senyshyn *et al.* (2009), (*g*) Vasylechko *et al.* (2000), (*h*) Ubizskii *et al.* (1994), (*i*) Marti *et al.* (1994) and (*j*) Geller (1957).

limit for a systematic experimental error is in the lower $10^{-5}$ range (see also errors given in Table 2).

Beyond the possibility of existing systematic errors in the works published so far differences in the lattice parameters can be mediated by internal strains which are caused by the introduction of structural defects (*e.g.* dislocations), impurities (foreign atomic species) and vacancies (non-stoichiometry). The measured etch-pit density indicates that the density of threading dislocations is below $10^5$ cm$^{-2}$. Here, the distance between adjacent dislocations is sufficiently large so that the strain fields between neighbouring dislocations cannot overlap. As a result of missing overlapping the mean lattice parameters – as measured by X-ray diffraction – remain unchanged. Therefore, dislocations should have a negligible impact on the (mean) lattice parameters in our samples. It is worth noting here that most of the works published so far (see Table 2) have been performed with powder samples. However, owing to the very small dislocation density in our samples, we do not expect a large difference between the lattice parameters of powder samples (which primarily break up at structural defects) and single crystalline samples.

For the perovskite-type crystals under investigation in this study it is generally believed that crystal vacancies arising from a non-stoichiometry show the largest influence on the lattice parameters, while foreign impurities should only have a minor effect. Unfortunately, no detailed experimental and theoretical works have been undertaken yet on the influence of crystal non-stoichiometry on the lattice parameters in $SrTiO_3$, $DyScO_3$ and $NdGaO_3$. We will therefore try to discuss this problem in a more qualitative way. It is well known that perovskite-type oxides $ABO_3$ often exhibit vacancies on the $A$ and the O site. This has been shown, for example, by Velickov *et al.* (2007) for Ln scandates. They have determined the stoichiometry in $GdScO_3$, $DyScO_3$, $SmScO_3$ and $NdScO_3$, and found that substitution with vacancies on the $A$ and O site is responsible for the lanthanoid deficiency. High-vacancy concentrations on the $A$ and O site of typically a few per cent have been observed. Similar to Ln scandates, an oxygen and neodymium deficiency of typically a few per cent has also been observed for Czochralski grown $NdGaO_3$ crystals (Talik *et al.*, 2004).

Ullmann & Trofimenko (2001) have shown that the missing occupation of $A$ and O sites in perovskite-type oxides $ABO_3$ should lead to a decrease in the Goldschmidt tolerance factor $t$ (Goldschmidt, 1930). They have estimated the effective ionic radii of several highly defective perovskite-type oxides from experimental data and found a universal linear relationship between the tolerance factor $t$ and the effective free volume, independent of the structural modifications of the perovskite type and of the type of defects. As a result of their study they found that a reduction of the tolerance factor would lead to an increase in the unit-cell volume.

While the effect of non-stoichiometry on the unit-cell volume has been discussed in the literature we could hardly find studies on how the non-stoichiometry in perovskite-type oxides $ABO_3$ will explicitly modify the lattice parameters $a$, $b$ and $c$. Freedman *et al.* (2009) have calculated the effect of various defect types in cubic $SrTiO_3$ on the local and long-range scale and give explicit values for each defect type. The calculations predict a very small lattice expansion in the presence of strontium ($A$) and oxygen (O) vacancies. On the other hand, the presence of titanium ($B$) vacancies – which are expected to appear with much lower probability – would lead to a significantly larger lattice expansion. To our knowledge no comparative calculations have been performed yet for the orthorhombic crystals $DyScO_3$ and $NdGaO_3$. It would be, for example, interesting to examine whether vacancies on the $A$ and O site lead to a uniform increase of all lattice parameters $a$, $b$ and $c$. Small changes in the lattice parameters, $\Delta a/a$, $\Delta b/b$ and $\Delta c/c$, are related to a corresponding change in the unit-cell volume $\Delta V/V$ of

$$\Delta V/V = \Delta a/a + \Delta b/b + \Delta c/c. \qquad (10)$$

From (10) it can be seen that a relative change in the unit-cell volume is determined by relative changes of all three lattice parameters $a$, $b$ and $c$, and in the most general case these changes may also exhibit *different signs*. For example $\Delta V/V$ can be a positive number, with $\Delta c/c > 0$ even if $\Delta a/a < 0$ and $\Delta b/b < 0$.

It is very instructive to compare our experimental results for the lattice parameters and unit-cell volumes with those from other groups (Table 2). Although the unit-cell volumes reported in these works vary within a comparatively large interval, it is striking that the relative deviations ($\Delta a/a$, $\Delta b/b$, $\Delta c/c$) of our data from the data of other works always exhibit the same sign. This behaviour is also reflected when comparing the unit-cell aspect ratios $a/b$, $a/c$ and $b/c$ as obtained in our work with those from other groups (Table 3). Surprisingly, only very small changes are observed. We can therefore conclude that a reduction/increase of the unit-cell volume caused by changes in the crystal stoichiometry is always

accompanied by a reduction/increase of all three lattice parameters *a*, *b* and *c*.

It has to be kept in mind that the discussion above is based on the assumption that systematic errors can be neglected in former studies and substantial changes in the crystal stoichiometry are responsible for the observed differences in the lattice parameters. In order to clarify this accurate lattice parameter measurements are needed on samples grown under different growth conditions leading to, for example, crystals with varying oxygen content. From these measurements the impact of non-stoichiometry on the lattice parameters may be studied more systematically. These extensive investigations go beyond the scope of the present study and are planned in the future.

## 5. Conclusions

In summary we have determined the lattice parameters of highly perfect $SrTiO_3$, $DyScO_3$ and $NdGaO_3$ single crystals at $293 \pm 0.5$ K. This has been achieved by applying a sophisticated high-resolution X-ray diffraction technique which is based on the modified Bond method and which uses both the rocking angle $\omega$ of the sample as well as the scattering angle $2\theta$. An accuracy of order of $10^{-5}$ has been achieved. Distinct differences in the lattice parameters and unit-cell volumes as compared to other works are observed. Since perovskite-type oxides $ABO_3$ often exhibit vacancies on the *A* and the O site these differences might be caused by intrinsic defects in the crystals. However, a detailed comparison with results from other works indicates that the differences in the *a*, *b* and *c* lattice parameters published by others could also be caused by systematic experimental errors.

We thank R. Uecker for valuable discussion and for providing us with the $DyScO_3$ single crystals.

## References


Abramov, Yu. A., Tsirelson, V. G., Zavodnik, V. E., Ivanov, S. A. & Brown I. D. (1995). *Acta Cryst.* B**51**, 942–951.

Als-Nielsen, J. & McMorrow, D. (2001). *Elements of Modern X-ray Physics.* New York: Wiley.

Ayers, J. & Ladell, J. (1988). *Phys. Rev. A*, **37**, 2404–2407.

Bartels, J. (1983). *J. Vac. Sci. Technol. B*, **1**, 338–345.

Biegalski, M. D., Dörr, K., Kim, D. H. & Christen, H. M. (2010). *Appl. Phys. Lett.* **96**, 151905.

Boikov, Y. A. & Claeson, T. (2001). *J. Appl. Phys.* **89**, 5053–5059.

Bond, W. L. (1960). *Acta Cryst.* **13**, 814–818.

Brous, J., Fankuchen, I. & Banks, E. (1953). *Acta Cryst.* **6**, 67–70.

Choi, K. J., Biegalski, M., Li, Y. L., Sharan, A., Schubert, J., Uecker, R., Reiche, P., Chen, Y. B., Pan, X. Q., Gopalan, V., Chen, L. Q., Schlom, D. G. & Eom, C. B. (2004). *Science*, **306**, 1005–1009.

Clark, J. B., Richter, P. W. & du Toit, L. (1978). *J. Solid State Chem.* **23**, 129–134.

Dirsyte, R., Schwarzkopf, J., Schmidbauer, M., Wagner, G., Irmscher, K., Bin Anooz, S. & Fornari, R. (2011). *Thin Solid Films*, **519**, 6264–6268.

DuMond, J. W. M. (1937). *Phys. Rev.* **52**, 872–883.

Dunn, C. G. & Koch, E. F. (1957). *Acta Metall.* **5**, 548–554.

Eerenstein, W., Wiora, M., Prieto, J. L., Scott, J. F. & Mathur, N. D. (2007). *Nat. Mater.* **6**, 348–351.

Fewster, P. F. (1999). *J. Mater. Sci. Mater. Electron.* **10**, 175–183.

Fewster, P. F. & Andrew, N. L. (1998). *Thin Solid Films*, **319**, 1–8.

Freedman, D. A., Roundy, D. & Arias, T. A. (2009). *Phys. Rev. B*, **80**, 064108.

Geller, S. (1957). *Acta Cryst.* **10**, 243–248.

Gesing, T. M. (2011). Personal communication.

Goldschmidt, V. M. (1930). *Naturwissenschaften*, **18**, 999–1013.

Haeni, J. H. *et al.* (2004). *Nature*, **430**, 758–761.

Härtwig, J., Hölzer, G., Wolf, J. & Förster, E. (1993). *J. Appl. Cryst.* **26**, 539–548.

Henke, B. L., Gullikson, E. M. & Davis, J. C. (1993). *At. Data Nucl. Data Tables*, **54**, 181–342.

Jeon, J.-H., Je, J. H. & Kang, S.-J. (1998). *J. Am. Ceram. Soc.* **81**, 624–628.

Kaganer, V. M., Brandt, O., Trampert, A. & Ploog, K. H. (2005). *Phys. Rev. B*, **72**, 045423.

Liferovich, R. P. & Mitchell, R. H. (2004). *J. Solid State Chem.* **177**, 2188–2197.

Lytle, F. W. (1964). *J. Appl. Phys.* **35**, 2212–2215.

Marimoto, T., Hidaka, O., Yamakawa, K., Arisumi, O., Kanaya, H., Iwamoto, T., Kumura, Y., Kunishima, I. & Tanaka, S. (2000). *Jpn. J. Appl. Phys.* **39**, 2110–2113.

Marti, W., Fischer, P., Altorfer, F., Scheel, H. J. & Tadin, M. (1994). *J. Phys. Condens. Matter*, **6**, 127–135.

Moram, M. A., Barber, Z. H. & Humphreys, C. J. (2007). *J. Appl. Phys.* **102**, 023505.

Rietveld, H. M. (1969). *J. Appl. Cryst.* **2**, 65–71.

Schuster, M. & Göbel, H. (1995). *J. Phys. D*, **28**, A270–A275.

Senyshyn, A., Trots, D. M., Engel, J. M., Vasylechko, L., Ehrenberg, H., Hansen, T., Berkowski, M. & Fuess, H. (2009). *J. Phys. Condens. Matter*, **21**, 145405.

Sim, J. S., Zhao, J. S., Lee, H. J., Lee, K., Hwang, G. & Hwang, C. S. (2006). *J. Electrochem. Soc.* **153**, C777–C786.

Talik, E., Kruczek, M., Sakowska, H., Ujima, Z., Gala, M. & Neumann, M. (2004). *J. Alloys Compd.* **377**, 259–267.

Tkach, A., Okhay, O., Vilarinho, P. M. & Kholkin, A. L. (2008). *J. Phys. Condens. Matter*, **20**, 415224.

Ubizskii, S. B., Vasylechko, L. O., Savytskii, D. I. & Matkovskii, A. O. (1994). *Supercond. Sci. Technol.* **7**, 766–772.

Uecker, R., Velickov, B., Klimm, D., Bertram, R., Bernhagen, M., Rabe, M., Albrecht, M., Fornari, R. & Schlom, D. G. (2008). *J. Cryst. Growth*, **310**, 2649–2658.

Uecker, R., Wilke, H., Schlom, D. G., Velickov, B., Reiche, P., Polity, A., Bernhagen, M. & Rossberg, M. (2006). *J. Cryst. Growth*, **295**, 84–91.

Ullmann, H. & Trofimenko, N. (2001). *J. Alloys Compd.* **316**, 153–158.

Vasylechko, L., Akselrud, L., Morgenroth, W., Bismayer, U., Matkovskii, A. & Savytskii, D. (2000). *J. Alloys Compd.* **297**, 46–52.

Velickov, B., Kahlenberg, V., Bertram, R. & Bernhagen, M. (2007). *Z. Kristallogr.* **222**, 466–473.

Yuan, G. L. & Uedono, A. (2009). *Appl. Phys. Lett.* **94**, 132905.